INVESTIGATION OF A MINIATURIZED CAPILLARY ISOELECTRIC FOCUSING (cIEF) SYSTEM USING A FULL-FIELD DETECTION APPROACH

Amy E. Herr, Joshua I. Molho
Juan G. Santiago, and Thomas W. Kenny
Mechanical Engineering Department, Stanford University
Stanford, CA 94305-4021

David A. Borkholder, Gregory J. Kintz,
Phillip Belgrader, M. Allen Northrup
Cepheid
Sunnyvale, California

ABSTRACT

Sample handling in miniaturized bioanalytical instruments typically depends on pressure or electrokinetic effects. This is particularly true of post-separation detection processes where a sample is moved past a single point detector. In contrast to such methods, the present study investigates a separation system that takes advantage of a steady-state, stationary separation technique known on the macroscale as capillary isoelectric focusing (cIEF). Due to the stationary nature of the final separation, sample analysis is conducted entirely without mobilization. This work explores the merits and limitations associated with miniaturizing this technique. Analyses were conducted on fluorescent peptide and protein samples in miniaturized separation columns (capillaries and glass micromachined channels between 8 and 14 mm long). In the interest of developing overall system portability, blue light emitting diodes (LED's) were used for sample excitation. Detection was accomplished using a charge-coupled device (CCD). This approach yielded complete multi-sample separations in less than 1 minute.

INTRODUCTION

Miniaturization of biochemical analysis systems has been investigated for several years, as researchers attempt to enhance the performance of specific separation systems. Performance, cost, and overall system throughput has been predicted to improve with shrinking channel dimensions[1]. Systems developed using micro electro-mechanical systems technologies have enabled further miniaturization of the complete analysis system.

Capillary isoelectric focusing (cIEF) relies upon equilibrium between the diffusion and electrophoresis of a species within pH and voltage gradients to accomplish separations (see Fig. 1). In cIEF, individual species are driven to a stationary location within the separation column that corresponds to the isoelectric point (pI, the pH at which the net charge on the sample goes to zero) of the respective species. This equilibrium behavior results in a high density of tightly-focused sample species spatially distributed within the separation column[2].

Traditional cIEF relies on a dual-stage separation scheme. The first stage consists of sample focusing, while the second stage relies on a chemical, hydrodynamic, or electroosmotic mobilization scheme. The necessity of this second stage arises from efforts to perform cIEF in instruments originally designed for electrophoresis. Such instruments make use of a single point detector at the end of the separation column. Thus, sample mobilization, in the case of cIEF, does not take advantage of the stationary, steady state characteristics of the final separation.

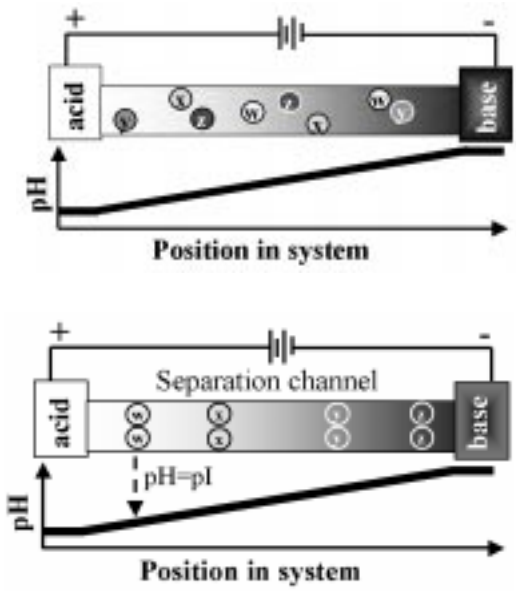

Figure 1. Schematic of cIEF separation. (top) *A pH gradient stabilized with a solution of ampholytes (represented by the white/black color gradient) has been established in the separation column. The protein samples, represented by the circles w-z, are distributed throughout.* ***(bottom)*** *An applied axial electric field causes the proteins to elecrophoretically migrate to the column position where the local pH equals the pI of the protein.*

Several studies [3,4] have used small separation column lengths for cIEF, but have sacraficed overall system portability by relying on bulky excitation sources. Significant reductions in column length (from a typical length of 30 cm to that of 4-5 cm) have permitted the entire separation column to be imaged via a full-field detector such as a CCD[5]. This allows for the collection of detailed spatial and temporal information. This method of detection also significantly shortens the analysis time[6] and virtually eliminates mobilization-related dispersion, as the second-stage of the traditional dual-stage approach is entirely omitted. This work explores some of the limits in the miniaturization of cIEF and investigates the performance of a miniaturized prototype system.

THEORY

cIEF Model

In cIEF, a mixture of protein samples is subjected to a strong electric field in a medium designed to have a linear pH gradient. At the molecular level, samples electrophoretically migrate along the channel until they reach the point in the pH gradient that is equal to their isoelectric pH (pI), where the protein no longer has a net charge. At the pI, the electrophoretic force on the protein due to the applied electric field is zero. Once the separation is complete and all samples have reached their respective isoelectric points, the separation is simply a stationary spatial distribution.

After the protein samples have "focused" at their isoelectric point locations, a steady-state equilibrium is achieved between electrophoresis and diffusion. In this final stage, the distribution of the protein band is determined by the opposing forces of diffusion (which tends drives proteins away from their pI locations) and an electrophoretic force that restores proteins toward their pI locations. This balance between electrophoresis and sample diffusion can be described by:

$$C\mu E = D\frac{dC}{dx} \tag{1}$$

with C as the sample concentration; μ, the electrophoretic mobility; E, the applied field strength; D, the diffusion coefficient of the species; and dC/dx, the concentration gradient. For simplicity, assume that the pH gradient, d(pH)/dx, and the mobility slope, dμ/d(pH), are constant within the small interval associated with a focused protein sample, this differential equation yields a modified Gaussian solution for the concentration distribution at steady state given by:

$$C(x) = C_o \exp[\frac{-x^2}{2\sigma^2}] \tag{2}$$

where σ in Eq. 2 is:

$$\sigma = \pm\sqrt{\frac{D}{E}\frac{dx/d(pH)}{-d\mu/d(pH)}} \tag{3}$$

As the values of the free parameters (i.e., d(pH)/dx, E) increase, the width of the distribution decreases.

Resolving Power

Resolving power for a particular cIEF system, be it macro- or microscale, is simply the minimum allowable proximity of two focused neighboring zones. The definition commonly used relates the inflection points (0.61 of the concentration maximum) of two identical neighboring Gaussian curves to the concentration minimum between the two concentration maxima. Svensson[7] proposed that when the curves are 3σ apart, the aforementioned concentration minimum is as deep as the inflection points on the Gaussian curves making this a resolvable sample separation (Fig. 2).

Using this criterion, the minimum pH separation between adjacent zones can be described as:

$$\Delta(pH)_{\min} = (\Delta L)_{\min}\frac{d(pH)}{dx} = 3\sigma\frac{d(pH)}{dx} \tag{4}$$

To determine the resolving power[8], set ΔpH equal to ΔpI and replace σ with Eq. (3):

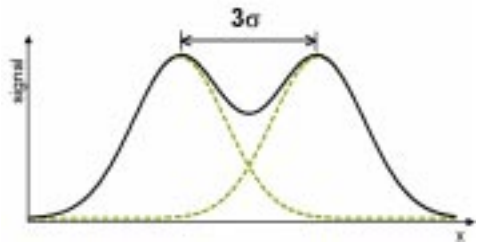

Figure 2. Minimum resolution of equivalent neighboring Gaussian peaks. *The solid line shows the sum of the two peaks, the dashed lines show the individual distributions.*

$$\Delta(pI)_{\min} = 3\sqrt{\frac{D}{E}\frac{(dpH/dx)}{(-d\mu/d(pH))}} \tag{5}$$

Substituting in the definition of the applied electric field strength, E = ϕ/L, in terms of applied potential, ϕ, and the length of the separation channel, L, and assuming that ϕ is held constant, the minimum resolvable pI difference is given by:

$$\Delta(pI)_{\min} = 3\sqrt{\frac{D}{(-d\mu/d(pH))}\frac{(dpH)}{\phi}} \tag{6}$$

Thus the minimum resolvable isoelectric point difference between adjacent focused bands is approximately independent of L and dependent only upon the individual protein characteristics, the total pH difference across the separation channel, and the applied potential. This channel length independence hypothesizes significant column miniaturization with minimal loss in the separation system performance. The limit to such miniaturization is probably determined by a maximum current density which, in turn, determines the maximum allowable temperatures and temperature gradients in the system. This effect is discussed below.

Temperature Considerations

Holding the applied potential constant while shrinking the length of the separation column (as in the discussion above) will increase the field strength and, thus, lead to increased Joule heating within the separation column. Such heating effects can cause otherwise plug-like sample bands to experience enhanced diffusion near the channel centerline because of local changes in viscosity. Such sample dispersion can limit the resolving power of miniaturized cIEF separation, as neighboring samples zones 'merge' into one another.

Researchers have investigated the effects of temperature gradients on other separation schemes, namely capillary electrophoresis[9] . This investigation is concerned with sample dispersion as a function of temperature. Assuming steady-state operation, only radial temperature variation, and an isotropic thermal conductivity, the heat conduction equation is given by:

$$\frac{1}{r}(\frac{d}{dr})(r\frac{dT}{dr}) = -\frac{\dot{q}}{k} \tag{7}$$

where r is the radial direction, T is the temperature, $\dot{q}$ is the heat generation rate, and k is the thermal conductivity. Integrating this equation and applying a constant surface temperature boundary condition, results in a solution for the temperature distribution:

$$T(r) = T_o + \frac{\dot{q}(r_o)^2}{4k}[1-(\frac{r}{r_o})^2] \tag{8}$$

where r_o is the inner radius of the separation channel, in this example 50 μm. Note that, in some cases, the assumption of fixed wall temperature may not be valid but serves here to demonstrate the effects of temperature-gradient-driven dispersion. This analysis estimates the temperature dependence of the viscosity[10] to be:

$$\eta_{r=o} \approx \eta_o exp[a + b(\frac{T_{r=r_o}}{T_{r=o}}) + c(\frac{T_{r=r_o}}{T_{r=o}})^2] \qquad (9)$$

where T_o = 273K, η_o = 0.001792 kg/(m sec), and a = -1.94, b = -4.80, and c = 6.74. Making use of the Nernst-Einstein equation, $D=\mu RT$, relates the mobility, $\mu=\varepsilon\zeta E/\eta$, and the temperature to the diffusivity of the sample. Where ε is the permitivity of the buffer, ζ is the zeta-potential, and E is the applied field strength. This describes how the diffusivity of the sample in a miniaturized cIEF system compares to that in a benchmark macroscale system (see Table 1).

Due to the exponential nature of the temperature dependence of the viscosity, channels less than 1 mm in length experience a rapid increase in the centerline diffusivity. So, as the separation channel is shortened below 1 mm, this analysis predicts significant sample blending. The choice of channel length investigated in this study (8 mm) avoids this significant centerline dispersion, yet allows for rapid separations and full-field imaging.

Miniature cIEF: Separation Channel Length (cm)	**Comparison with Macroscale cIEF: Increase in Diffusivity (% Increase in $D_{centerline}$)**
10.0	< 0.1
0.5	4
0.1	23

Table 1. Joule heating and diffusivity. *Comparison of centerline diffusivity for a miniaturized system (channel lengths given in the first column) to that of a macroscale system (channel length is 20 cm). Both cases are for a 50 μm channel radius. The applied potential is held constant and all sample parameters are the same for each case.*

Other limitations to the miniaturization of the cIEF system exist. Among these are the absolute temperature rise with respect to the surrounding and the performance of the detection system. The former limitation is concerned with the maximum temperature in the system and is a strong function of the size of the cross-sectional geometry of the separation column and the thermal properties of the capillary walls and sample holder. In turn, the maximum allowable temperature is a function of the type of protein that is used. The later consideration has significant impact on the design for portability of the miniaturized system. These limitaions will be explored in detail in future work.

EXPERIMENTAL APPARATUS

No work at present addresses the need for portability of the entire cIEF system: separation channel, excitation source, and detection scheme. Previous works utilize a CCD detector and a miniaturized separation channel, but rely on lasers for fluorescence excitation. For example, Pawliszyn[3] investigated a non-mobilized system composed of an array detector, 4-5 cm long separation channel, and an Argon ion laser. The lasers employed are bulky and require cooling. This work investigates the performance of an excitation system based on a compact (3 mm in diameter), low-power (~240 mW), inexpensive (less than $5 each) LED source (Chicago Miniature; Hackensack, New Jersey).

The prototype non-mobilized system consists of an array detector, an 8 mm separation column (Polymicro Technologies, Tempe, Arizona) permanently mounted between fluid reservoirs, and an LED array excitation source (see Fig. 3). UV-curable refractive index matching epoxy (Norland Optical Adhesives, New Brunswick, New Jersey) was used to affix the column to the Delrin (DuPont; Wilmington, Delaware) cartridge. These short columns, compared to tens of centimeters in traditional cIEF, can be imaged and simultaneously monitored until the optimum separation is achieved.

The fused-silica channels were cleaned and prepared prior to each separation. The channels were rinsed for 5 min. with a 1 M NaOH solution, followed by a 5 min. 20 mM NaOH solution rinse. To suppress electroosmotic flow (EOF), a neutral EOF-suppressing polymer, in this case a 0.4% solution of methylcellulose, was then rinsed through the channel for 5 min. and allowed to equilibrate in the channel for approximately 15 min. Proper EOF suppression is critical[11] for a non-mobilized system.

Proposed sample detection techniques involving cIEF suggest that fluorescence detection increases detection limits over more traditional schemes based on UV detection, as UV absorbing ampholytes interfere with sample detection[12]. In the present study, fluorescently-tagged peptides were prepared and diluted to the appropriate concentrations with ampholytes (Bio-Rad CE-IEF Ampholytes 3/10)[4]. The sample mixture was then injected into the prepared capillary cartridge. The reservoirs in the capillary cartridge were filled with basic catholyte (20mM NaOH) or acidic anolyte (10mM H_3PO_4). The cartridge was placed in the miniaturized system, platinum electrodes were inserted into each reservoir, and a potential (0 kV-2 kV) was applied. A CCD camera (Hamamatsu S7034-0907) with PC interface was used to acquire real-time spatial intensity distribution information (Fig. 4).

RESULTS AND DISCUSSION

Hydrodynamic Mobilization

This full-field detection approach was used to extract information about the dispersion effects introduced through a pressure-driven sample mobilization. To accomplish this, samples were allowed to separate and were then mobilized by a slight pressure-driven flow (mobilization velocity of ~ 0.3 mm/sec) (see Fig. 5). The electric field was maintained during sample mobilization, so as to minimize sample dispersion due to diffusion (this approach is often applied in macroscale systems).

By the time the sample was mobilized out of the short separation channel, the overall width of the sample had increased significantly. An estimate of the number of plates, N, obtainable in the hydrodynamically-mobilized system (see Fig. 6) was based upon a skewed peak model developed by Foley and Dorsey[13]. While the hydrodynamic mobilizaiton velocity used in this study is on the same order of that traditionally used in macroscale systems (i.e., u ~ 0.3 mm/sec vs. u ~ 0.1 mm/sec), the loss in system efficiency is likely to be exaggerated as compared to macroscale cIEF. This arises from the fact that this investigation was conducted in free solution; whereas macroscale cIEF is often performed in a gel matrix. The gel acts to resist the pressure-driven flow, hence a direct comparison of efficiency between the two schemes is not appropriate. The overall dispersive trends, however, are illustrutive and indicate the existance of enhanced sample band dispersion due to mobilization. The efficiency values do indicate directly that such hydrodynamic mobilization in a miniature cIEF free solution system utilizing a single-point detector would significantly reduce the system performance.

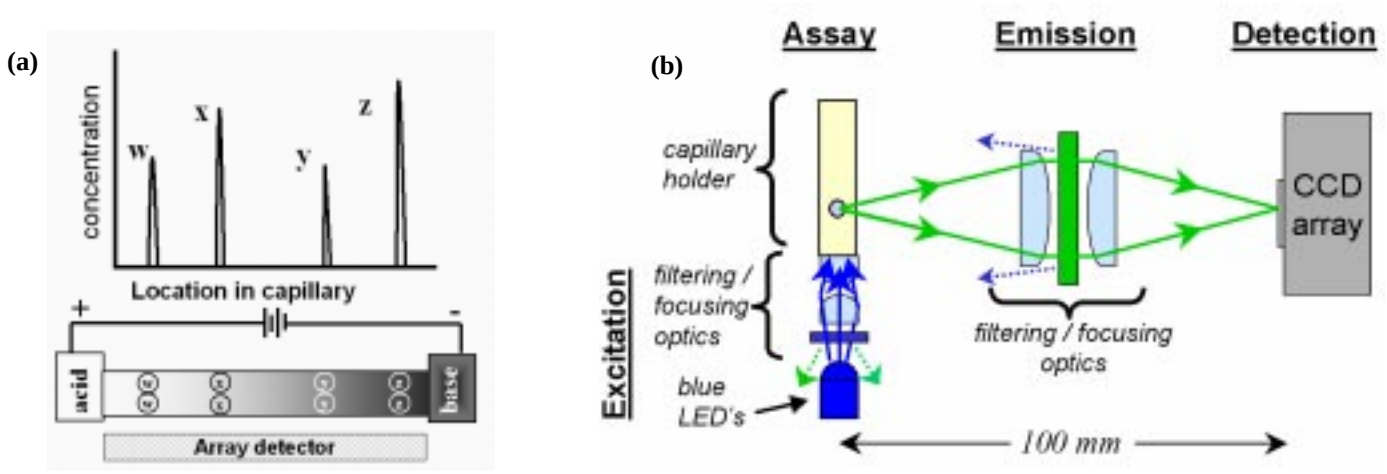

Figure 3. Schematic of protein-fluorescence array detection. *An axial electric field has been applied, resulting in the formation of an axial pH gradient within a background field of ampholytes (represented by the white/black color gradient). Proteins initially distributed homogeneously in the column migrate to their respective pI location (represented by circles w-z).* ***(a)*** *Concentration/intensity vs. spatial location information is obtained from the detection system.* ***(b)*** *A series of blue LEDs provide excitation for fluorescently-tagged proteins in a cIEF assay. The emission is then focused onto a CCD array that is then vertically binned.*

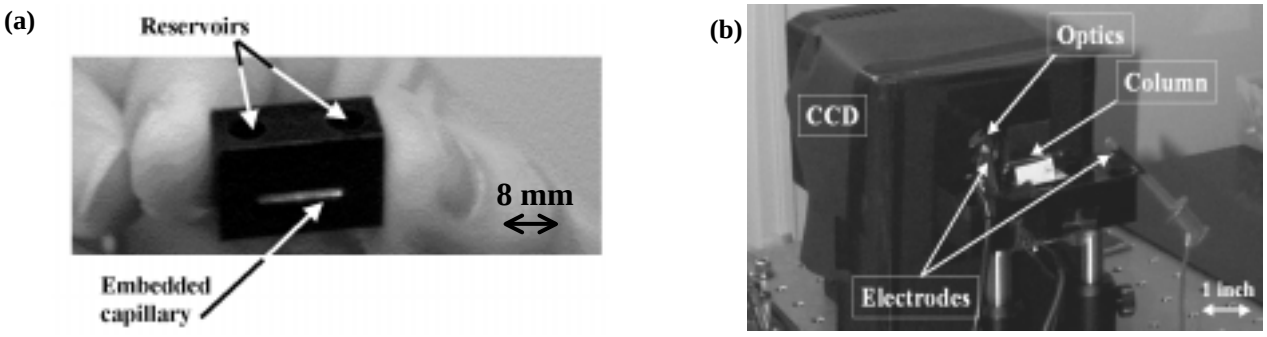

Figure 4. Miniaturized IEF System. ***(a)*** *Capillary cartridge and* ***(b)*** *the hardware mount for the excitation source and optics, the cartridge mount, the emission filtering/focusing optics, and the CCD detection component of the diagnostic are shown.*

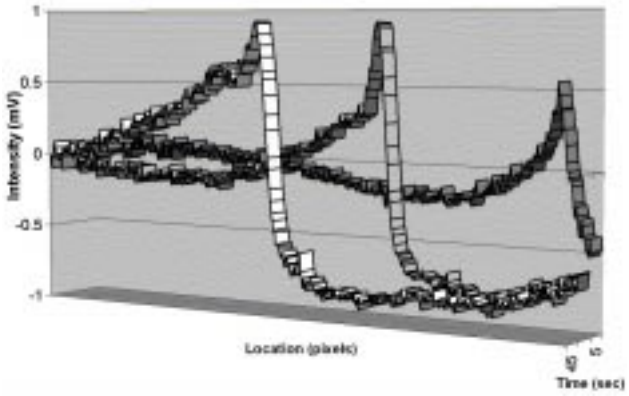

Figure 5. Effect of hydrodynamic mobilization of a single protein. *Hydrodynamic mobilization (u ~ 0.3 mm/sec) of 100 nM protein sample. The protein is focused and pressure-driven flow has been applied for (from back to front) 5 sec. (Δt_p = 5s), 25 sec., and 45 sec. The sample moves out the end of the column where a single point detector would potentially be located. Capillary I.D. 75μm, O.D. 360μm, and length 8 mm*

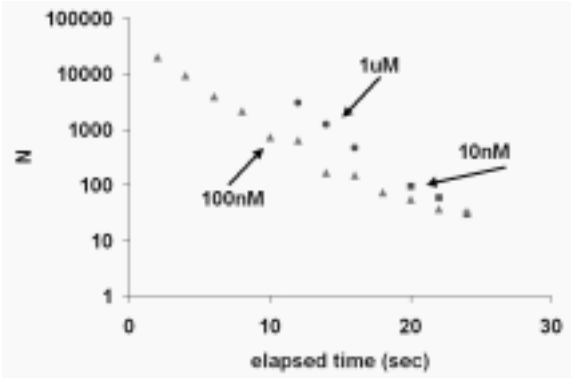

Figure 6. Effects of hydrodynamic mobilization on the number of plates (N) attainable. *Protein samples were focused and subsequently mobilized through the separation column using pressure driven flow. The width of a given peak was measured and N was calculated. This initial data shows a degradation in the system performance as the sample moves past an imaginary single point detector. The real-time, array detector approach allows us to image such dynamic processes.*

Multi-Sample Separation

The short separation column (8 mm) in the prototype cIEF system allows the entire column to be imaged; thus, enabling the separation to be monitored continuously and captured when it has reached steady state. Figure 7 illustrates this approach, showing a complete separation of two peptides taking place in less than one minute, compared to tens of minutes for traditional cIEF.

After steady-state is achieved, the separation remains stable exhibiting the profile dipicted in Fig. 7 for tens of minutes. The two sample peaks are separated by 5σ (using the σ of the wider peak, Peak 1) and are, thus, quite easily resolved. This quality agrees well with the previous resolving power analysis, as peaks separated by more than 3σ should be readily resolvable. Also, consideration of the initial temperature gradient analysis suggests that there is limited Joule heating (less than 3% more than would be predicted for a 200 cm long separation channel) in this system.

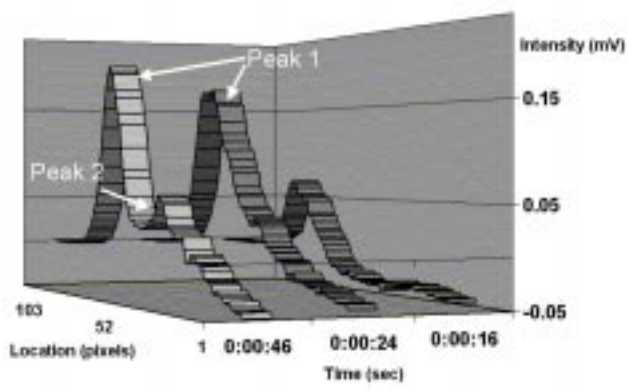

Figure 7. Array detection of a cIEF separation of two fluorescently tagged protiens. *The separation column was filled with a homogenous mixture of ampholytes (BioLyte CE-IEF Ampholytes 3/10) and 500 nM sample. One reservoir was filled with an acid (pH 2); the other was filled with a base (pH 10). Upon application of the electric field, (16 sec) the samples start to focus into one peak. (24 sec) A small second peak is moving right and separates from the major peak at approximately 46 sec. Two peaks are then clearly resolved. The estimated pH separation was calculated to be ΔpH = 0.65 pH units. E = ~ 500 V/cm, capillary I.D. 75μm, O.D. 360μm, and length 8 mm.*

CONCLUSIONS

The short (8 mm) separation columns used in this miniaturized cIEF system allow for real-time, full-field imaging of the complete separation process with a CCD. This point is of particular importance as traditional cIEF relies on a two-stage sample analysis protocol: the sample separation and mobilization of the sample past a point detector. During any mobilization scheme, diffusion and distortion of the separated sample bands may occur, resulting in degraded system performance. Thus, the full-field imaging system allows for less degradation in the final system resolution, as mobilization is unnecessary.

This prototype miniaturized cIEF system allows for the study of various system parameters (e.g., the applied field strength, axial pH gradient, and assay characteristics) on the overall separation efficiency. This system consisted of a short separation column permanently mounted between fluid reservoirs with LED-based fluorescence excitation and CCD detection. Initial work with this prototype system investigated fundamental principles of cIEF, including the resolving power of a cIEF system and temperature gradient considerations limiting the miniaturization of the separation component of the system. This work successfully demonstrates rapid multi-component sample separations in less than 1 minute using the miniature full field imaging system.

ACKNOWLEDGEMENTS

The authors wish to thank the Defense Advanced Research Projects Agency (DARPA) Contract No. N65236-98-1-5414 (Cepheid), DARPA Contract No. F33615-98-1-2853 (Stanford University). Financial support for A.E. Herr and J.I. Molho is provided by the National Science Foundation's Graduate Research Fellowship and the Hewlett-Packard-Stanford University Graduate Fellowship Programs, respectively.

REFERENCES

1. A. Manz et al., "Planar Chips Technology for Miniaturization of Separation Systems: A Developing Perspective in Chemical Monitoring", *Advances in Chromatography*, **33** (1993), 2-66.
2. P.G. Righetti, *Immobilized pH Gradients: Theory and Methodology* (Amsterdam: Elsevier, 1990).
3. X.-Z. Wu, J. Wu, and J. Pawliszyn, "Fluorescence imaging detection for capillary isoelectric focusing", *Electrophoresis*, **16** (1995), 1474-1478.
4. K.A. Cruickshank, J. Olvera, and U.R. Muller, "Simultaneous Multiple Analyte Detection Using Fluorescent Peptides and Capillary Isoelectric Focusing", *Journal of Chromatography A*, **817** (1998), 41-47.
5. J. Wu and J. Pawliszyn, "Absorption Spectra and Multicapillary Imaging Detection for Capillary Isoelectric Focusing Using a Charge Coupled Device Camera", *Analyst*, **120** (1995), 1567-1571.
6. Q. Mao and J. Pawliszyn, "Capillary isoelectric focusing with whole column imaging detection for analysis of proteins and peptides", *Journal of Biochemical and Biophysical Methods*, **39**, no. 1-2, (1999), 93-110.
7. H. Svensson, *J. Chromatogr.*, **25** (1966), 266-273.
8. H. Rilbe, "Theoretical Aspects of Steady-State Focusing," in *Isoelectric Focusing*, ed. N. Catsimpoolas (New York: Academic Press, 1976), 13-52.
9. E. Grushka, R. M. McCormick, and J.J. Kirkland, "Effect of Temperature Gradients on the Efficiency of Capillary Zone Electrophoresis Separations", *Anal. Chem.*, **61** (1989), 241-246.
10. F.M. White, *Fluid Mechanics* (San Francisco: McGraw-Hill, Inc, 1994).
11. M. Minarik et al., "Dispersion Effects Accompanying Pressurized Zone Mobilization in Capillary Isoelectric Focusing of Proteins", *Journal of Chromatography A*, **738** (1996), 123-128.
12. G.F. Verbeck and S.C. Beale, "Isoelectric Point Analysis of Proteins and Peptides by Capillary Isoelectric Focusing with Two-Wavelength Laser-Induced Fluorescence Detection", *J. Microcolumn Separations*, **715** (1999), 708-715.
13. J. P. Foley and J. G. Dorsey, "Equations for Calculation of Chromatographic Figures of Merit for Ideal and Skewed Peaks", *Analytical Chemistry*, **55**, no. 4, (1983), 730-737.